Brazed Joint Properties and Microstructure of SCS-6/ß21S Titanium Matrix Composites

Delamination-dominated failure modes indicate interlaminar shear strength of the composite limits performance of joints fabricated with Ti-Cu-Ni-based filler metals

BY E. K. HOFFMAN, R. K. BIRD, AND D. L. DICUS

ABSTRACT. The properties and microstructure of brazed joints of SCS-6 SiC fiber reinforced ß21S (Ti-15Mo-2.7Nb-3Al-0.2Si, wt-%) titanium matrix composite (TMC) were investigated. Brazed joint specimens were fabricated from TMC using two different forms of commercially available Ti-15Cu-15Ni braze filler metal. The brazed joint specimens were tested in air at room temperature and 1500°F (815°C) using overlap tensile shear (OLTS) tests. Metallurgical and fractographic analyses were used to characterize the microstructure, brazing filler metal/TMC interactions, and joint failure modes. The fractographic results indicated that TMC delamination is a dominant failure mode for this type of joint. At room temperature, the TMC brazed joint specimens failed by TMC delamination and TMC tensile failure, with the brazed joint remaining intact. Therefore, the performance of the brazed joint specimens at room temperature is limited by the interlaminar strength of the TMC and not by the braze strength. At 1500°F, the TMC brazed joint specimens exhibited a combination of delamination and braze shear failure. Thus, the high-temperature performance of the brazed joint specimens may be limited by both the TMC interlaminar properties and the strength of the braze.

E. K. HOFFMAN and R. K. BIRD are Materials Engineers and D. L. DICUS is a Senior Research Engineer with the Materials Division, NASA Langley Research Center, Hampton, Va.
Paper presented at the 24th International AWS Brazing and Soldering Conference held April 27-29, 1993, in Houston, Tex.

Introduction

The performance goals for future hypersonic vehicles require the development of new, low density materials with improved elevated-temperature properties which can be incorporated into highly efficient structural airframe components (Ref. 1). Fiber-reinforced titanium matrix composites (TMC) offer significant specific strength and stiffness advantages and enhanced elevated-temperature performance over their monolithic counterparts and are prime candidates for hot structure applications at temperatures up to 1500°F (815°C). One specific TMC system, ß21S (Ti-15Mo-2.7Nb-3Al-0.2Si, wt-%) titanium alloy reinforced with continuous SCS-6 SiC fibers (henceforth designated as SCS-6/ß21S TMC), is of particular interest based upon its elevated-temperature strength and stiffness, thermal and environmental stability in a hypersonic service environment, fiber/matrix compatibility, and fabricability (Ref. 2).

KEY WORDS

Brazing
Titanium MMC
SCS-6/ß21S Composite
Ti-Cu-Ni Filler Metal
Joint Properties
High Temp. Performance
Microstructure
Fractography
TMC Delamination
Interlaminar Strength

The development of joining processes capable of incorporating TMC into efficient structural components is essential to the successful deployment of hypersonic vehicles. Previous research showed that brazing is a viable process for fabricating TMC structural components and that Ti-15Cu-15Ni brazing filler metal has the potential to produce TMC brazed joints with reasonable T-joint strengths at temperatures up to 1500°F (Ref. 3). In addition to producing adequate brazed joint strength, the braze process itself must not degrade the TMC properties. Additional research has indicated that the Ti-15Cu-15Ni brazing filler metal does not affect the fiber/matrix interface (Ref. 4); the room-temperature, 1200°F (650°C), and 1500°F TMC tensile properties (Ref. 4); or the room-temperature TMC fatigue life (Ref. 5).

Extensive characterization of the brazing process for TMC must be undertaken to provide preliminary design allowables for TMC brazed structure operating in a hypersonic environment and give confidence for use of such materials and fabrication technologies. Hence, the evaluation of brazed TMC joint properties at expected service temperatures will be required.

This study was undertaken to investigate the properties and microstructure of brazed joints of $[0/90]_s$ and $[0/\pm45/90]_s$ laminates of SCS-6/ß21S TMC fabricated using two different forms of commercially available Ti-15Cu-15Ni brazing filler metal. Brazed joint properties were

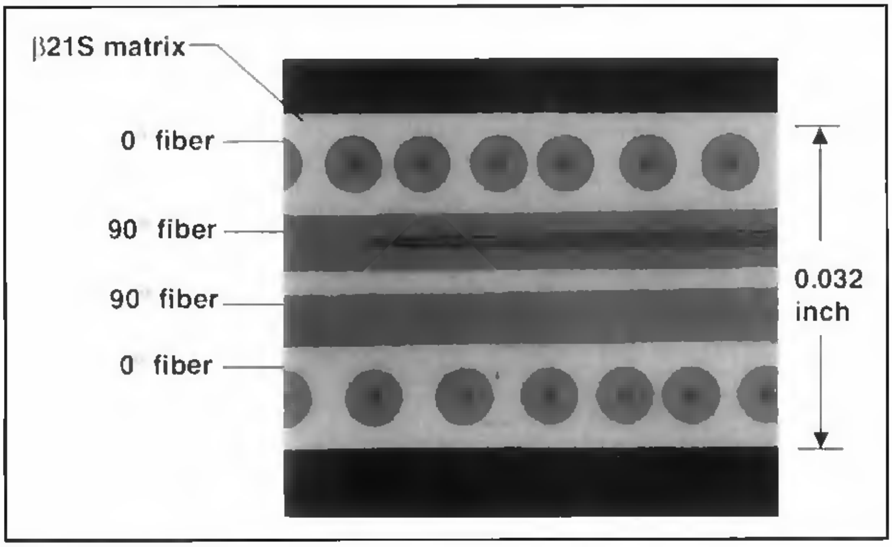

Fig. 1 — Cross section of $[0/90]_s$ SCS-6/β21S TMC laminate.

evaluated at room temperature and 1500°F using overlap tensile shear (OLTS) tests. Metallurgical and fractographic analyses were used to characterize the microstructure, brazing filler metal/TMC interactions, and joint failure modes.

Experimental

Materials

The matrix alloy used was β21S of nominal composition Ti-15Mo-2.7Nb-3Al-0.2Si (wt-%). This alloy is a metastable beta alloy (beta transus ($T_β$) ~ 1460°F, 793°C) requiring a stabilization heat treatment prior to use. The β21S matrix was reinforced with continuous SCS-6 SiC fibers. The SCS-6 fiber, which is produced by Textron Specialty Materials, consists of stoichiometric SiC deposited on a carbon monofilament core. A graded, carbon-rich SiC protective outer coating is applied in a separate operation to control reaction with the titanium alloy matrix during elevated-temperature exposure and to prevent fiber damage during handling. The fiber has a nominal diameter of 0.0056 in. (142 µm). The SCS-6 fibers were fabricated in the form of unidirectional mats with Ti-Nb wire crossweave used to hold the fibers in place.

The composite was manufactured by Textron Specialty Materials using a foil-fiber-foil approach in which alternating layers of 0.0045-in. (0.114-mm) thick β21S foils and SCS-6 fiber mats were consolidated into laminates by hot isostatic pressing. The TMC used in this study were 0.032-in. (0.813-mm) thick, 4-ply $[0/90]_s$ and 0.064-in. (1.626-mm) thick, 8-ply $[0/\pm45/90]_s$ laminates. A typical cross-section showing the $[0/90]_s$ SCS-6/β21S TMC laminate lay-up is shown in Fig. 1. The nominal fiber volume fraction for each laminate was 0.39.

Two different commercially available product forms of Ti-15Cu-15Ni brazing filler metal were evaluated: Ticuni[1] and MBF-5003[2].

Ticuni is a clad-laminated brazing filler metal (LBFM) foil produced by WESGO. The foil strip is produced by co-rolling a 50/50 copper-nickel alloy sheet between two sheets of commercially pure titanium. The relative proportions of sheet thickness are controlled so as to produce a final composition of Ti-15Cu-15Ni. The Ti-15Cu-15Ni LBFM was supplied as foil strip 4 in. in width by 0.003 in. in thickness (101.6 by 0.076 mm). MBF-5003 is a rapidly solidified amorphous brazing filler metal (ABFM) foil produced by Allied-Signal, Metglas Products. The Ti-15Cu-15Ni ABFM was supplied as foil strip 0.5 in. in width by 0.0015 in. in thickness (12.7 by 0.038 mm). Table 1 shows the solidus and liquidus temperatures for these brazing filler metals. The homogeneity of the Ti-15Cu-15Ni ABFM causes melting to occur over a narrower temperature range and at lower temperatures than those for the Ti-15Cu-15Ni LBFM (Ref. 6).

Table 1 — Solidus and Liquidus of Ti-15Cu-15Ni LBFM and ABFM Brazing Filler Metals

Brazing Filler Metal	Solidus, °F (°C)	Liquidus, °F (°C)
LBFM	1670 (910)	1760 (960)
ABFM	1656 (902)	1710 (932)

Overlap Tensile Shear Specimens

The TMC brazed joint shear behavior was evaluated with double OLTS specimens, which were machined from larger double OLTS panels. Previous work with single OLTS specimens indicated that the specimens failed in the TMC near the joint interface due to bending stresses developed during loading as the brazed joint attempted to align with the load axis. The double OLTS specimen design was selected to minimize the effect of these bending moments. Figure 2 shows a schematic diagram of an OLTS panel assembly prior to braze processing. The center legs measured 1.5 in. in length by 2.5 in. in width (38.1 by 63.5 mm), and the outer legs measured 0.6 in. in length by 2.5 in. in width (15.2 by 63.5 mm). The legs were oriented so that the loading axis was parallel to the 0-deg fiber direction. The larger overlap joint B had greater load-carrying capacity than the smaller overlap joint A, thereby ensuring that joint A would fail first.

The panels were prepared by placing a 0.003-in. (0.076-mm) thick layer of brazing filler metal within the faying surfaces of each overlap region. (Double layers of 0.0015-in.-thick foil were used for the Ti-15Cu-15Ni ABFM.) The braze foil extended 0.13 in. (3.3 mm) past the edges of the overlaps. This small excess helped provide additional material to form fillets at the overlap edges and to seal the faying surfaces. Stainless steel foil straps were resistance tack welded to the panel edges of the overlap regions and the panels were deadweight loaded to 1 psi (6.9 kPa) pressure to fixture the assembly for brazing. Following brazing, the fixturing straps were removed and the panels were diamond wheel saw cut into OLTS specimens measuring 0.5 in. (12.7 mm) wide.

Various overlap distances (OL) were evaluated for joint A in order to determine the overlap-to-thickness (OL/t) ratio at which brazed joint shear failure occurs. Previous work with monolithic β21S indicated an OL/t ratio of 1 would be necessary to produce braze shear failure (Ref. 7). Since 0.063 in. (1.6 mm) represents the smallest overlap that can be readily produced, OLTS specimens fabricated with 0.032-in. (0.81-mm) thick $[0/90]_s$ TMC can have a minimum OL/t ratio of approximately 2. In order to estimate brazed joint shear behavior at smaller OL/t ratios, thicker TMC material

1 Ticuni® is a registered trademark of WESGO, Inc.
2 METGLAS® Braze Foil (MBF) is a registered trademark of Allied-Signal, Inc., Metglas Products.

Table 2 — Ti-15Cu-15Ni LBFM and ABFM Brazing Processing Parameters

Brazing Filler Metal	Processing Parameters: Braze Step	Diffusion Soak	Stabilization Age
LBFM	$T > T_L$ 25 min	$T_L > T > T_S$ 2 h	$T < T_\beta$ 8 h
ABFM	$T > T_L$ 25 min	—	$T < T_\beta$ 8 h

T_L = liquidus
T_S = solidus
T_β = beta transus

must be used. Therefore, OLTS specimens were fabricated from 0.032-in.-thick $[0/90]_s$ TMC with OL/t ratios of 2 and 4 and from 0.064-in.-(1.63-mm-) thick $[0/\pm45/90]_s$ TMC with OL/t ratios of 1 and 2.

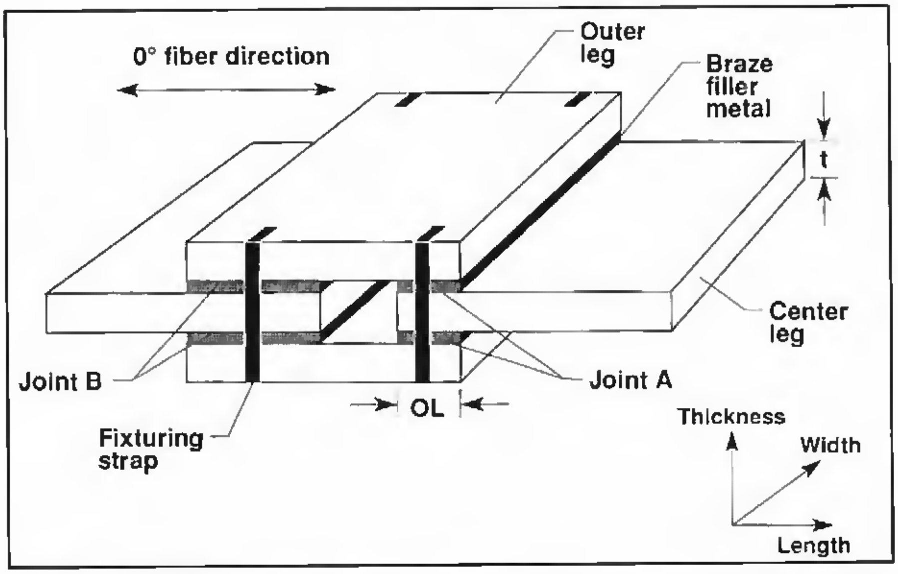

Fig. 2 — Schematic diagram of overlap tensile shear panel assembly prior to braze processing.

Brazing Procedure

In preparation for braze processing, the TMC pieces were chemically cleaned with a commercial detergent, rinsed with deionized (DI) water, etched in a nitric-hydrofluoric bath, rinsed with DI water, and hot air dried. The brazing filler metals were degreased with acetone.

The brazing filler metals required different thermal processes due to the differences in their product forms and liquidus temperatures (Ref. 3). The thermal processes used for the two brazing filler metals are shown in Table 2. The Ti-15Cu-15Ni LBFM diffusion soak was used to homogenize the brazing filler metal/base metal microstructure. A diffusion soak was not included in the ABFM thermal process due to the homogeneity of the brazing filler metal. The stabilization heat treatment, which took place during cool down from the braze step or diffusion soak temperatures, was used to stabilize the ß21S properties for extended elevated-temperature service (Ref. 8) and to prevent brittle ω phase formation in the ß21S at intermediate service temperatures (Ref. 9).

Thermal processing was conducted in an electrically heated vacuum furnace at a vacuum better than 10^{-5} torr (1.3 mPa). The panels were heated at a rate of 30°F/min (17°C/min) to approximately 150°F (83°C) below the braze step temperature. The furnace temperature was held at that level for 15 min to permit the panel and furnace temperatures to equilibrate. The panels were then heated at a rate of 10°F/ min (6°C/min) to the brazing step temperature. Following the 25 min brazing step hold time, the panels were furnace cooled to the respective diffusion soak and stabilization heat treatment temperatures. After the stabilization heat treatment, the brazed panels were furnace cooled to ambient temperature.

Mechanical Testing

The OLTS tests were conducted in air at room temperature and 1500°F in accordance with ANSI/AWS C3.2-82 (Ref. 10). Four replicate specimens were tested at each temperature unless otherwise noted. Tests were conducted with a servo-hydraulic test machine using hydraulic grips designed for use at both room and elevated temperatures. For the elevated-temperature tests, the specimens and grips were heated using a three-zone, split tube furnace. A thermocouple was attached to the specimens in the vicinity of the brazed joint to monitor specimen temperature. The heat-up time was approximately 1 h, and the specimens were allowed to soak at the test temperature for 5 min prior to loading. Joint temperature uniformity was ±3°F (±2°C) for the duration of the test. The specimens were loaded to failure at an actuator displacement rate of 0.010 in./min (0.25 mm/min).

Two stress values were calculated for each OLTS specimen: the shear stress (τ) developed in brazed joint A at failure and the tensile stress (σ) developed in the TMC center leg at failure. These stresses are represented by the following equations:

$$\tau = P_{max}/[2(OL \cdot w)] \quad (1)$$

$$\sigma = P_{max}/(w \cdot t) \quad (2)$$

where P_{max} is the maximum load applied to the specimen, OL is the joint A overlap distance, w is the width of the specimen, and t is the thickness of the center leg.

Metallurgical Analyses

Brazed joint microstructures were characterized using optical microscopy and scanning electron microscopy (SEM). Metallurgical specimens were cross-sectioned using diamond saw cutting and mounted in an epoxy medium. Following polishing, the specimen surfaces were etched using Kroll's re-agent. Brazed joint fracture surfaces were examined using optical and SEM microscopy.

Results and Discussion

Metallurgical Analyses

Figures 3A and 3B show representative microstructures of brazed joints from $[0/\pm45/90]_s$ TMC OLTS specimens fabricated with Ti-15Cu-15Ni LBFM and ABFM, respectively. The microstructures of the brazed joints are characterized by a central band of acicular structure with a single phase ß-Ti region on either side of the acicular band. The microstructure of the stabilized ß21S matrix remote from the brazed joint is characterized by acicular α-Ti phase precipitated within the ß-Ti grains and by α-Ti phase decorating the grain boundaries.

The acicular bands were much thicker than the original 0.003-in. (76-µm) filler metal thickness, averaging 0.0066 in. (168 µm) thick for the Ti-15Cu-15Ni LBFM joints and 0.0052 in. (132 µm) thick for the Ti-15Cu-15Ni ABFM joints. The thickness of the acicular bands represents the brazing filler metal plus ß21S matrix that melted and/or underwent solid-state transformation to a multiphase structure during braze processing. The thickness of the single phase ß-Ti zones in the ß21S matrix adjacent to the Ti-15Cu-15Ni LBFM joints was noticeably greater than that of the corresponding zones adjacent to the Ti-15Cu-15Ni ABFM joints. In the Ti-15Cu-15Ni LBFM joints, these single-phase ß-Ti zones typically extended to the nearest layer of SCS-6 fibers. The thicker acicular bands and the thicker single-phase ß-Ti zones in the Ti-15Cu-15Ni LBFM specimens were attributed to the higher temperatures and longer times associated with the Ti-15Cu-15Ni LBFM braze thermal process.

The phase equilibria diagram for the Ti-Cu-Ni system (Ref. 11) indicates that a ternary eutectic reaction occurs at 1650°F (900°C) at the Ti-10Cu-20Ni composition. The solid eutectic phases are ß-Ti, Ti_2Cu (ε), and Ti_2Ni (δ). Based on the phase diagram, proeutectic ß-Ti and ε phases formed during cooling from the Ti-15Cu-15Ni LBFM brazing step temperature to the diffusion soak temperature. Upon continued cooling to the stabilization heat treatment temperature, the remaining liquid at the braze joint centerline solidified, forming the eutectic mixture of ß-Ti, ε and δ phases.

Figure 4 shows high-magnification SEM photomicrographs and EDS analyses of the brazed joint region from Fig. 3A. The higher magnification view shows the central portion of the acicular band. The acicular structure is a mixture of the dark-colored proeutectic phases and the light-colored eutectic phases. Point 1 is a large precipitate of proeutectic ß. Point 2 is a mixture of the eutectic phases and is representative of the last liquid to solidify. Due to the fine structure of the acicular band, individual chemistries of the precipitates could not be determined. The acicular structure becomes finer toward the outer edges of the acicular band. X-ray diffraction analyses verified that the brazed joint region containing the acicular band and the areas adjacent to the band consisted of α- and ß-Ti with minor amounts of ε and δ (Ref. 4). The Cu and Ni concentration gradients from the center to the edges of the acicular band (Points 3–5) indicate that the brazing filler metal constituents are well diffused. Point 6 lies within the single-phase ß-Ti zone in the ß21S matrix. In this zone, the concentration of the ß-Ti stabilizers (Mo, Nb, Cu, and Ni) was high enough to suppress α-Ti formation during the stabilization heat treatment. In addition, the concentration of Cu and Ni was low enough that the intermetallics ε and δ did not form, resulting in a zone of single-phase ß-Ti. At larger distances from the brazed joint centerline, the concentration of Cu and Ni became progressively lower so that the α-Ti phase formed first as decorations along the ß-Ti grain boundaries followed by general precipitation within the ß-Ti grains near

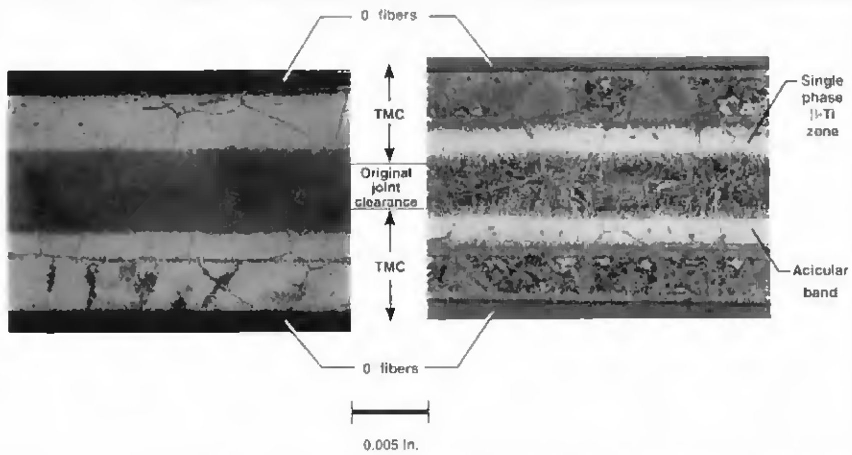

Fig. 3 — Microstructure of [0/±45/90]$_s$ SCS-6/ß21S TMC brazed joints fabricated with: A — Ti-15Cu-15Ni LBFM; B — Ti-15Cu-15Ni ABFM brazing filler metals.

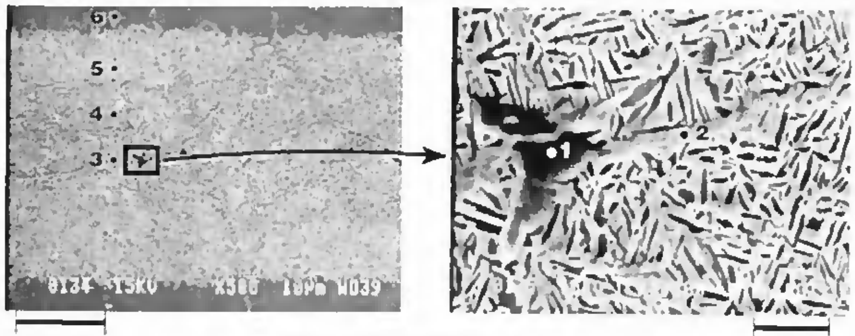

Concentration, weight percent

Point	Ti	Mo	Nb	Al	Cu	Ni
1	98.0	0.1	0.8	0.0	0.6	0.6
2	62.0	0.6	0.6	0.0	26.2	10.6
3	78.3	5.2	1.7	0.5	8.3	6.1
4	76.3	6.0	1.8	0.5	8.9	6.5
5	79.1	9.1	2.4	0.6	4.8	4.1
6	77.3	12.7	3.0	0.9	2.7	3.3

Fig. 4 — Microstructure and EDS analysis of [0/±45/90]$_s$ SCS-6/ß21S TMC brazed joint fabricated with Ti-15Cu-15Ni LBFM.

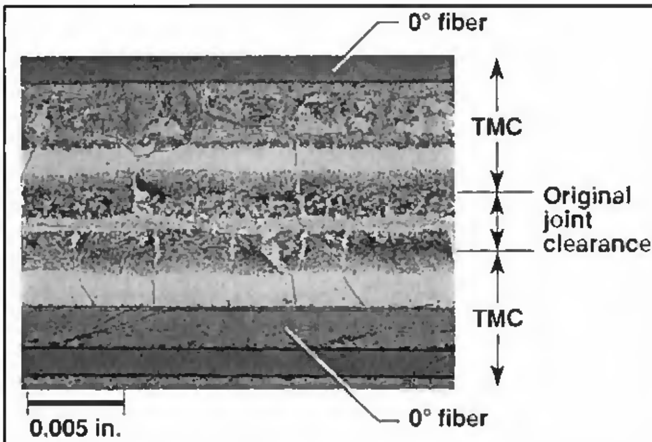

Fig. 5 — Microstructure of [0/±45/90]$_s$ SCS-6/ß21S TMC brazed joint fabricated with Ti-15Cu-15Ni ABFM.

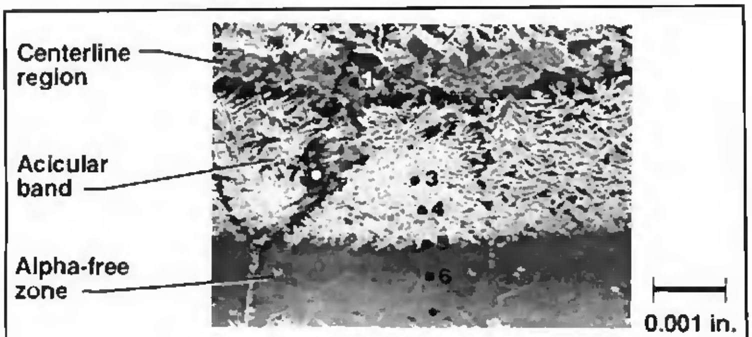

Concentration, weight percent

Point	Ti	Mo	Nb	Al	Cu	Ni
1	60.5	0.8	2.0	0.3	22.2	13.7
2	77.4	9.6	4.0	0.5	2.5	5.4
3	77.5	4.7	2.8	0.8	7.9	5.9
4	68.9	9.2	3.8	0.9	9.3	7.5
5	72.9	14.1	4.8	1.3	2.9	3.5
6	74.2	14.0	5.1	1.7	1.7	2.9
7	62.1	2.1	2.2	0.3	8.2	24.8

Fig. 6 — Microstructure and EDS analysis of $[0/\pm45/90]_s$ SCS-6/ß21S TMC brazed joint fabricated with Ti-15Cu-15Ni ABFM.

the SCS-6 fibers of the TMC — Fig. 3A.

The Ti-15Cu-15Ni ABFM specimens displayed more variation in the thickness and morphology of the acicular band than did the Ti-15Cu-15Ni LBFM specimens. Figure 5 shows the microstructure of a brazed joint fabricated with Ti-15Cu-15Ni ABFM in which a continuous, light-colored region formed along the centerline and grain boundaries of the acicular band. In contrast, Fig. 3B shows only small, dispersed areas of the same color. (Note that Figs. 5 and 3B are different sections from a single specimen.) The distribution of this light-colored region varied from isolated areas to a continuous band, and appeared to be concentrated in the thicker sections of the joint. The thickness of the acicular band in Fig. 5 is 0.0054 in. (137 µm) as compared to an acicular band thickness of 0.0045 in. (114 µm) in Fig. 3B.

Figure 6 shows a high-magnification SEM photomicrograph and EDS x-ray chemical analyses of a portion of the brazed joint shown in Fig. 5. In the continuous, centerline region (Point 1), the Cu and Ni concentrations were comparatively high. This centerline region represents residual liquid that solidified on cooling and its composition is similar to that in the Ti-15Cu-15Ni LBFM specimen (Point 2 in Fig. 4). The continuous residual liquid regions appeared to form in thicker sections of the joint due to joint mismatch and variations in fit-up tolerances. Points 2–5 represent the proeutectic phases in the acicular band. These phases become finer toward the outer edges of the acicular band. Point 6 represents the single phase zone in the ß21S matrix. The concentration profiles of the acicular band and single-phase zone in the Ti-15Cu-15Ni ABFM specimen are similar to those of the Ti-15Cu-15Ni LBFM specimen shown in Fig. 4. A Ni-rich phase (Point 7) of a different composition than the centerline region formed along a grain boundary.

In those sections of the Ti-15Cu-15Ni ABFM joint that exhibited the continuous centerline residual liquid regions, the braze processing parameters were insufficient to completely diffuse the excess liquid into the matrix. These regions were more prevalent for the Ti-15Cu-15Ni ABFM specimens due to the lower braze step temperatures and absence of the diffusion soak. At the higher temperatures and longer times associated with the Ti-15Cu-15Ni LBFM processing cycle, the centerline residual liquid region represents a small fraction of the braze joint volume.

Overlap Tensile Shear Tests

Figure 7 shows the room-temperature test results for the OLTS specimens fabricated with Ti-15Cu-15Ni LBFM and ABFM. The figure shows plots of the average shear stress developed in brazed joint at failure and the average tensile stress developed in the TMC center leg at failure as a function of the OL/t ratio. The scatter bars show the spread in the reported test data. The associated specimen failure modes at each OL/t ratio are also shown. Overall, these results indicate little difference in the OLTS performance for the two brazing filler metals regardless of laminate thickness or layup. However, different failure modes

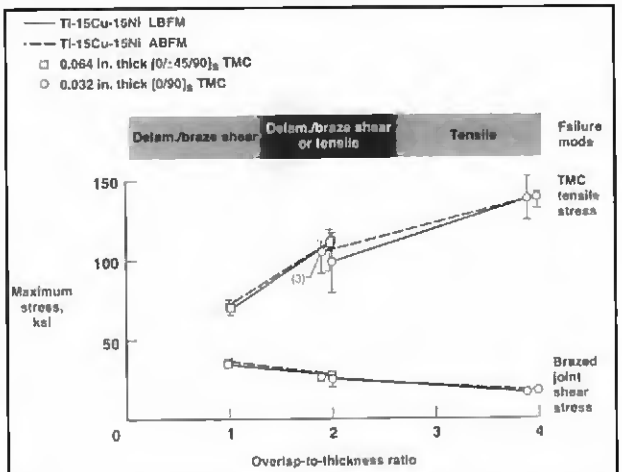

Fig. 7 — Effect of overlap-to-thickness ratio on room temperature performance of SCS-6/ß21S TMC Ti-15Cu-15Ni LBFM and ABFM brazed OLTS specimens. Four replicate tests, with exceptions noted in parentheses.

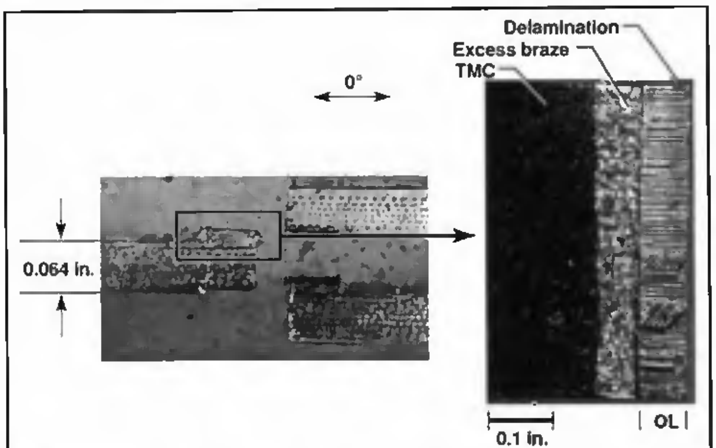

Fig. 8 — Room-temperature delamination failure of $[0/\pm45/90]_s$ SCS-6/ß21S TMC Ti-15Cu-15Ni LBFM brazed OLTS specimen with OL/t of 1.

Table 3 — Average Strength of Monolithic ß21S Overlap Tensile Shear (OLTS) Joints Fabricated with Ti-15Cu-15Ni LBFM and ABFM Brazing Filler Metals (Ref. 7)

Braze Filler Metal	OL/t	OLTS Strength (ksi) RT	OLTS Strength (ksi) 1500°F
LBFM	1	53.2	>3.6[a]
ABFM	1	42.0	4.1

(a) Lower bound estimate, braze joint did not fail.

were observed in some cases.

At an OL/t ratio of 1, the $[0/\pm45/90]_s$ TMC specimens failed predominantly by TMC delamination at an average brazed joint shear stress of 36 ksi (248 MPa). This shear stress is significantly less than that achieved at room temperature with monolithic ß21S (Table 3).

At an OL/t ratio of 2, the $[0/\pm45/90]_s$ TMC specimens failed either by delamination or by TMC tensile failure. This inconsistency of failure mode indicates that, at an OL/t ratio of 2, the load required to fracture the $[0/\pm45/90]_s$ TMC is approximately equal to the load required to cause TMC delamination. The $[0/90]_s$ specimens failed either by delamination, tensile, or a combination of braze shear and delamination.

At an OL/t ratio of 4, the $[0/90]_s$ TMC specimens all failed by TMC tensile fracture at an average tensile stress of 139 ksi (958 MPa). The data indicate that an OL/t ratio between 2 and 4 was necessary to prevent room-temperature joint failure of the $[0/90]_s$ TMC specimens.

Figure 8 shows a typical room-temperature delamination failure for a $[0/\pm45/90]_s$ TMC Ti-15Cu-15Ni LBFM brazed OLTS specimen with an OL/t ratio of 1. Delamination occurred along the consolidation boundaries of various plies adjacent to the brazed joints, exposing fibers from the delaminated plies. The Ti-15Cu-15Ni ABFM brazed specimens with OL/t ratios of 1 exhibited a similar failure mode, although some of these specimens exhibited some distinct regions of braze shear. However, the predominate failure mode was still delamination and no specimen failed solely by braze shear.

Figure 9 shows the 1500°F test results for the TMC OLTS specimens fabricated with Ti-15Cu-15Ni LBFM and ABFM. All of these specimens failed by a mixture of TMC delamination and braze shear at shear stresses ranging from 2.4 to 4.2 ksi (17 to 29 MPa). These shear stresses are comparable to the brazed shear strengths achieved at 1500°F with monolithic ß21S (Table 3) and represent approximately 10% of the TMC braze shear stresses achieved at room temperature for similar laminates and OL/t ratios.

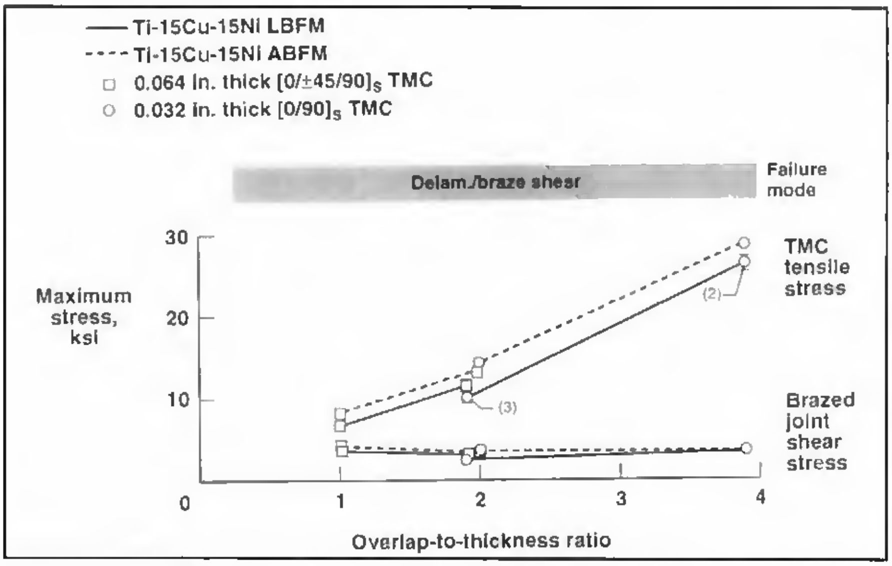

Fig. 9 — Effect of overlap-to-thickness ratio on 1500°F performance of SCS-6/ß21S TMC Ti-15Cu-15Ni LBFM and ABFM brazed OLTS specimens. Four replicate tests, with exceptions noted in parentheses.

TMC tensile failure was not observed in these tests due to the low brazed joint shear strength of Ti-15Cu-15Ni LBFM and ABFM at 1500°F. At an OL/t ratio of 4, the average tensile stress developed in the $[0/90]_s$ TMC specimens at failure was 27.7 ksi (191 MPa). Based on extrapolation of the data, an OL/t ratio of approximately 10 would be required to prevent joint failure (Ref. 7).

Figure 10 shows an example of the 1500°F delamination/braze shear failure of a $[0/90]_s$ TMC Ti-15Cu-15Ni LBFM brazed OLTS specimen with an OL/t ratio of 4. The figure shows the mating joint fracture surfaces and a schematic diagram indicating the location of the fracture path. TMC delamination occurred in the 0-deg plies adjacent to the brazed joint at the end of each outer leg and at the end of the center leg. In the center of the joint, the fracture path transitioned from the 0-deg plies into the braze, resulting in a region of braze shear failure. In general, the proportion of delamination to braze shear tended to be larger at larger OL/t ratios. The $[0/90]_s$ TMC Ti-15Cu-15Ni ABFM brazed OLTS specimens with OL/t ratios of 4 exhibited some variation in failure mode, however, the predominant failure mode was still delamination and braze shear.

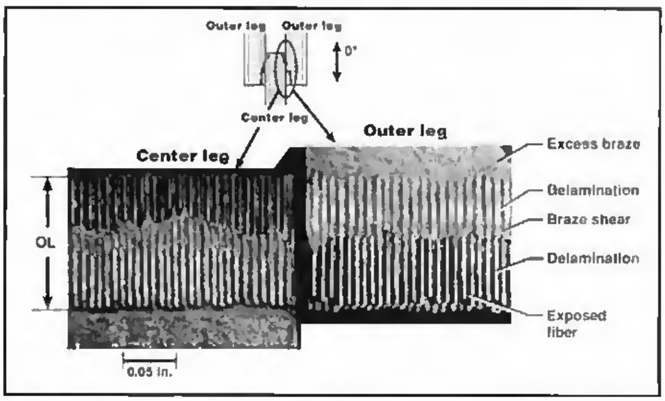

Fig. 10 — 1500°F delamination/braze shear failure of $[0/90]_s$ SCS-6/ß21S TMC Ti-15Cu-15Ni LBFM brazed OLTS specimen with OL/t of 4.

The cause of these delamination-dominated failure modes can be attributed to the relatively weak fiber/matrix interface (Ref. 12) coupled with the high peel stresses developed at the ends of the joints (Ref. 13). At room temperature, delamination occurred by interlaminar shear along the consolidation boundaries of the various plies adjacent to the brazed joint. In most cases, the brazed joint remained completely intact. At 1500°F, delamination occurred at the ends of the joint in the 0-deg plies adjacent to the braze due to high peel stresses. Toward the center of the joint, the peel stresses were reduced and the interlaminar shear strength of the composite exceeded the braze strength. As a result, the fracture path transitioned from the 0-deg plies into the braze, resulting in a region of braze shear failure.

The possibility exists that braze processing degrades the interlaminar shear strength of the composite. Previous analysis (Ref. 4) of the fiber/matrix interfaces near the joint showed that no Cu or Ni from the brazing filler metal had penetrated the protective C-rich SiC outer coating of the fibers and that only a limited amount of these elements had reached the fiber/matrix interface. In addition, the fiber/matrix reaction zone thickness was not affected by the thermal cycles associated with either braze process. Short beam flexural tests on a similar TMC system, uniaxial SCS-6/Ti-15-3 TMC, showed that the composite failed by interlaminar shear at a shear stress of 38 ksi (260 MPa) (Ref. 14). This measured interlaminar shear stress is consistent with the room-temperature TMC brazed joint shear stresses. Thus, braze processing does not appear to degrade the interlaminar shear strength of the composite.

These results indicate that the OLTS performance of the TMC brazed joints is limited by the interlaminar shear strength of the composite. At room temperature, the failure mode changes from TMC delamination at low OL/t ratios to tensile failure at high OL/t ratios. Thus, the brazed joints were strong enough to accommodate at least as much tensile and shear stress as the TMC and are, therefore, adequate for room-temperature service. At 1500°F, brazed joint specimens exhibited a mixture of TMC delamination and braze shear failure at all of the OL/t ratios tested. Thus, the high-temperature performance of the brazed joints may be limited by both the TMC interlaminar shear strength and the strength of the braze. Despite the influence of the interlaminar shear strength on TMC brazed joint shear behavior, the two braze processes produced adequate joint strength to permit useful TMC structures to be designed for application at temperatures up to 1500°F.

Conclusions

A study was conducted to evaluate the properties and microstructure of brazed joints of $[0/90]_s$ and $[0/\pm45/90]_s$ laminates of SCS-6 SiC fiber-reinforced ß21S titanium matrix composite (TMC). The brazed joints were fabricated using two different forms of commercially available Ti-15Cu-15Ni brazing filler metal: a laminated foil (Ti-15Cu-15Ni LBFM), and a rapidly solidified amorphous foil (ABFM). Brazed joint properties were measured at room temperature and 1500°F (815°C) using overlap tensile shear (OLTS) tests.

The OLTS test results indicated that TMC delamination is a dominant failure mode for this type of joint. At room temperature, the brazed joint specimens failed by TMC delamination and TMC tensile failure, with the brazed joint remaining intact. Therefore, the performance of the brazed joints at room temperature is limited by the interlaminar strength of the TMC and not by the braze strength. At 1500°F, the braze joint specimens exhibited a mixture of TMC delamination and braze shear failure. Thus, the high-temperature performance of the brazed joints may be limited by both the TMC interlaminar properties and the strength of the braze. Despite the influence of the interlaminar shear strength on TMC brazed joint shear behavior, the two braze processes produced adequate joint strength to permit useful TMC structures to be designed for application at temperatures up to 1500°F.

The overlap tensile shear test results were similar for the Ti-15Cu-15Ni LBFM and ABFM TMC specimens fabricated with the corresponding TMC laminates and OL/t ratios, although the failure modes differed in some cases. At room temperature, the failure mode changes from TMC delamination at low OL/t ratios to tensile failure at high OL/t ratios. The minimum OL/t ratio necessary to prevent joint failure at room temperature was determined to be between 2 and 4 for the $[0/90]_s$ TMC specimens. At 1500°F, the TMC specimens failed by braze shear and delamination at all the OL/t ratios tested and at approximately 10% of the room-temperature TMC braze shear stresses. The minimum OL/t ratio necessary to prevent joint failure at 1500°F was estimated to be 10 for the $[0/90]_s$ TMC specimens.

The Ti-15Cu-15Ni LBFM and ABFM brazed joint microstructures were characterized by a central band of acicular structure with a single-phase ß-Ti region on either side of the acicular band. The acicular band had high concentrations of Cu and Ni and consisted of α-Ti, ß-Ti, Ti_2Cu, and Ti_2Ni. The single-phase ß-Ti region resulted from the outward diffusion of the ß-Ti stabilizing elements, Cu and Ni, from the brazed joint. The Ti-15Cu-15Ni LBFM brazed joints had thicker acicular bands and thicker single-phase ß-Ti regions than those in the Ti-15Cu-15Ni ABFM brazed joints due to the higher temperatures and longer times associated with the Ti-15Cu-15Ni LBFM braze thermal process.

References

1. Tenney, D. R., Lisagor, W. B., and Dixon, S. C. 1988. Materials and structures for hypersonic vehicles. NASA Technical Memorandum 101501, October.

2. NASP Materials and Structures Augmentation Program Final Report. 1993. Titanium Matrix Composites, Volume I — Executive Summary, Program Summary and Requirements. NASP Contract Report 1145, Vol. 1, Contract F33657-86-C-2126, March.

3. NASP Materials and Structures Augmentation Program Final Report. 1993. Titanium Matrix Composites, Volume II — Material and Process Development. NASP Contract Report 1145, Vol. II, Contract F33657-86-C-2126, March.

4. Hoffman, E. K., Bird, R. K., and Dicus, D. L. 1994. Effect of braze processing on the microstructure and mechanical properties of SCS-6/ß21S titanium matrix composites. *Welding Journal* 73: 185-s to 191-s.

5. Dicus, D. L., Bird, R. K., Hoffman, E. K., and Wiedemann, K. E. 1993. Brazing and oxidation-resistant coating effects on tensile and fatigue behavior of ß21S titanium matrix composites. NASA Technical Memorandum 109030, December.

6. Rabinkin, A., Liebermann, H., Pounds, S., Taylor, T., Reidinger, F., and Siu-Ching Lui. 1991. Amorphous Ti-Zr-base Metglas® brazing filler metals. *Scripta Metallurgica*, Vol. 25, pp. 399–404.

7. Hoffman, E. K., Bird, R. K., and Dicus, D. L. 1994. Brazed joint properties and microstructure of SCS-6/ß21S titanium matrix composites. NASA Technical Paper 3396, May.

8. Niemann, J. T., and McAfee, J. L. 1991. Development of titanium matrix composites. *Tenth National Aero-Space Plane Technology Symposium*, Monterey, Calif. April 23–26, Paper No. 181.

9. Bowen, A. W. 1984. Omega phase formation in metastable ß-titanium alloys. *Beta Titanium Alloys in the 1980s*. R. R. Boyer and H. W. Rosenberg, eds. The Metallurgical Society of AIME, pp. 85–106.

10. *Standard Method for Evaluating the Strength of Brazed Joints in Shear.* 1982. ANSI/AWS Standard C3.2-82. American National Standards Institute/American Welding Society, Miami, Fla.

11. Shalin, R. E, and Kovneristy, Yu. K. 1980. Phase stability and phase equilibria in titanium alloys. *Titanium '80 Science and Technology*. H. Kimura and O. Izumi, eds. Proceedings of the Fourth International Conference on Titanium, Kyota, Japan, May 19–22, pp. 277–293.

12. Nimmer, R. P., Bankert, R. J., Russell, E. S., and Smith, G. A. 1990. Micromechanical modeling of fiber/matrix interface effects in SiC/Ti metal matrix composites. *Proceedings of the 13th Conference on Metal Matrix, Carbon, and Ceramic Matrix Composites*. NASA Conference Publication 3054, Part 2, pp. 493–514.

13. Hart-Smith, L. J. 1981. Further developments in the design and analysis of adhesive-bonded structural joints. *Joining of Composite Materials*, ASTM STP 749, K. T. Kedward, ed., ASTM, pp. 3–31.

14. Jansson, S., Deve, H. E., and Evans, A. G. 1991. The anisotropic mechanical properties of a Ti matrix composite reinforced with SiC fibers. *Metallurgical Transactions A*, Vol. 22A, pp. 2975–2984.